

Synthesis and mechanochemical inertness of a Zn (II) bidipyrin double helix

Junfeng Zhou | Devavrat Sathe | Andrew Ciccotelli | Junpeng Wang 

School of Polymer Science and Polymer Engineering, The University of Akron, Akron, Ohio, USA

Correspondence

Junpeng Wang, School of Polymer Science and Polymer Engineering, The University of Akron, Akron, OH 44325-3909, USA.
Email: jwang6@uakron.edu

Funding information

National Science Foundation, Grant/Award Number: CHE-2204079; Extreme Science and Engineering Discovery Environment, Grant/Award Number: TG-CHE220003

Abstract

Helices are unique structures that play important roles in biomacromolecules and chiral catalysis. The mechanochemical unfolding of helical structures has attracted the attention of chemists in the past few years. However, it is limited to a few cases which investigated how the mechanochemical reactivity is impacted by helical configurations. No synthetic helical mechanophore is reported. Herein, a Zn (II) bidipyrin (BDPR-Zn) double helix is designed as a potential mechanophore. A cyclic olefin containing a doubly strapped BDPR-Zn is prepared and used for ring-opening metathesis polymerization. The corresponding polymer is subjected to pulsed ultrasonication for mechanochemical testing. The sonication results reveal the mechanochemical inertness of BDPR-Zn unit, which is further supported by force-coupled simulation. Although no obvious activation is observed, our preliminary results on BDPR-Zn unit could inspire further rational designs on force-induced helix unfolding.

KEY WORDS

helix, mechanochemical unfolding, mechanochemistry, mechanophore, Zn (II) bidipyrin

1 | INTRODUCTION

Helices are extensively present in biological systems, such as proteins¹ and DNAs,² and this secondary structure is important in maintaining the function of the biomolecules and in storing genetic information. The unique structure–property relationship of helical structures has attracted the attention and interest of synthetic chemists. Synthetic polymers, with this helical secondary structure, show distinct properties and performances.^{3–8} Helical small-molecule catalysts^{9,10} and supramolecular assemblies^{11,12} have also been developed successfully.

A series of non-covalent interactions, such as hydrogen bonding¹³ and metal–ligand coordination,^{11,12} contribute to the formation of helical structures. A well-studied helical system is Zn (II) bidipyrin (BDPR-Zn, Figure 1A), which is formed by the reaction between Zn

(II) cation and linear bidipyrin dimer without additional counterions.^{14–20} The BDPR-Zn complex is stable in solution, making it convenient for spectroscopic characterization. Recently, Maeda and Muranaka prepared doubly strapped BDPR-Zn helices with different lengths of straps and systematically investigated two double helix modes (Figure 1B) and the spring-like behavior at different temperatures.¹⁷ They observed that long alkyl-strapped analogs exhibited *S* mode (short distance between two the Zn atoms); when the alkyl straps were replaced with butene, the helix exhibited *L* mode (long distance between two Zn atoms) as the predominant species. They attributed the change in the mode of helix to the rigid jack-like butene unit, which extended the pitch of the double helix.¹⁷ In addition, singly strapped double helices were found to be in the *S* mode because of the lack of one rigid strap. Importantly, the two modes show distinct

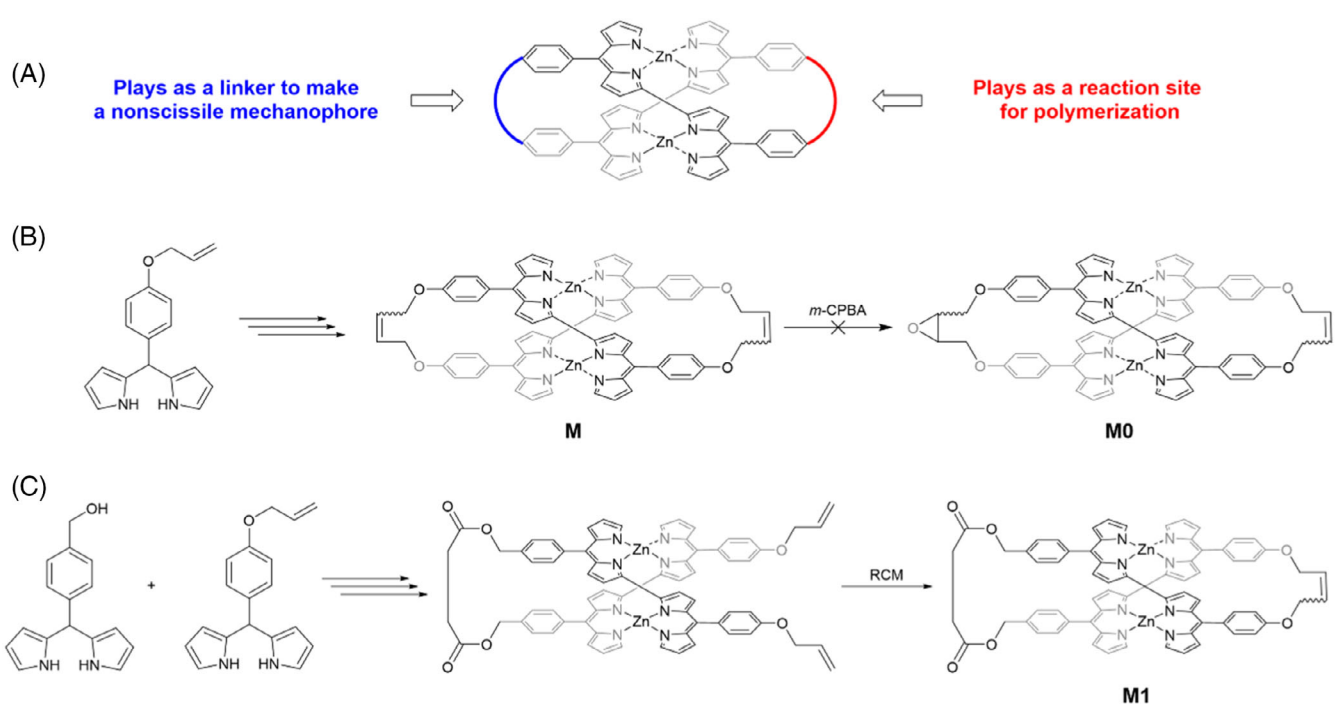
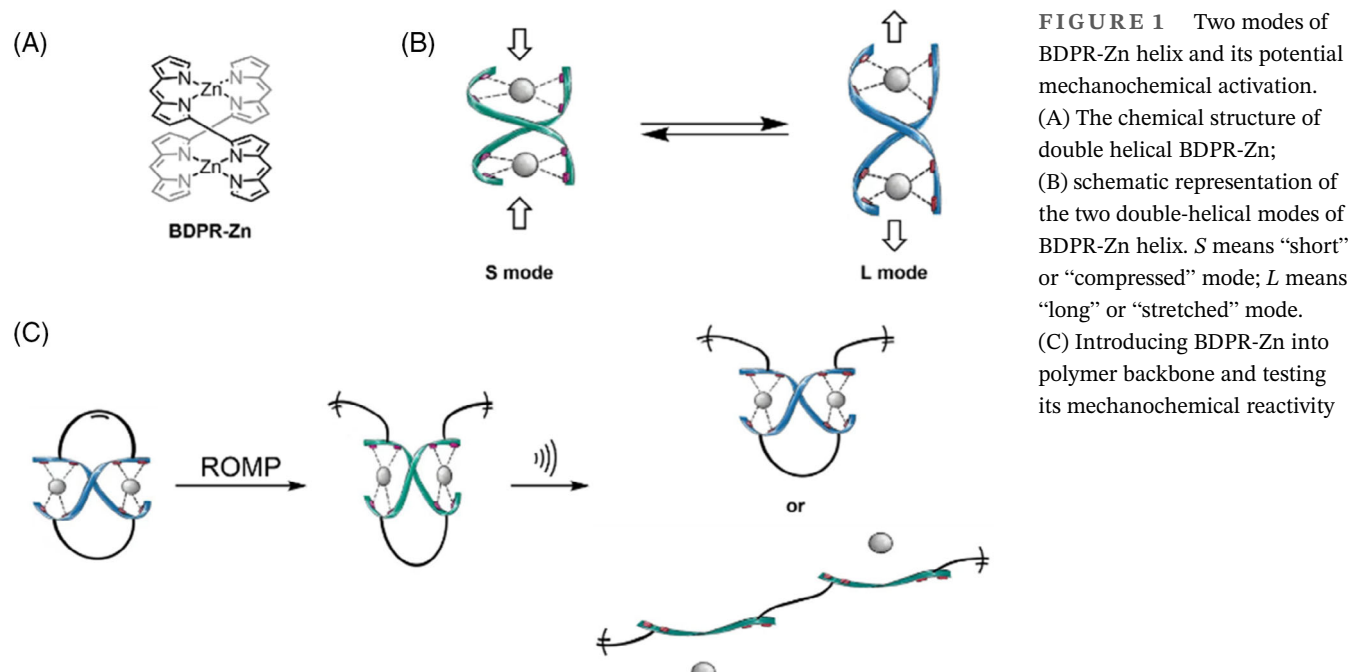


FIGURE 2 Desymmetrization of BDPR-Zn and helical macrocyclic monomer design. (A) The chemical structure design of BDPR-Zn helical monomer; (B) Desymmetrization through direct epoxidation of a symmetric BDPR-Zn cyclic diene failed to afford helical monomer M0; (C) helix monomer (M1) is prepared by using two phenyl dipyrromethanes with different functional groups as the starting materials

absorbance peaks in their UV-vis spectroscopy, which can be used to conveniently detect the conformation change.

Inspired by this work, we are interested in testing the response of the strapped BDPR-Zn helix under mechanical force. We hypothesize that mechanical force can

extend butene-strapped *S* mode helix to *L* mode and eventually break the metal-ligand bond to convert the helical structure into a linear one (Figure 1C). In this report, we explored the feasibility of using a BDPR-Zn strapped helix as a mechanophore. We synthesized a cyclic olefin that contains a BDPR-Zn helix, which was

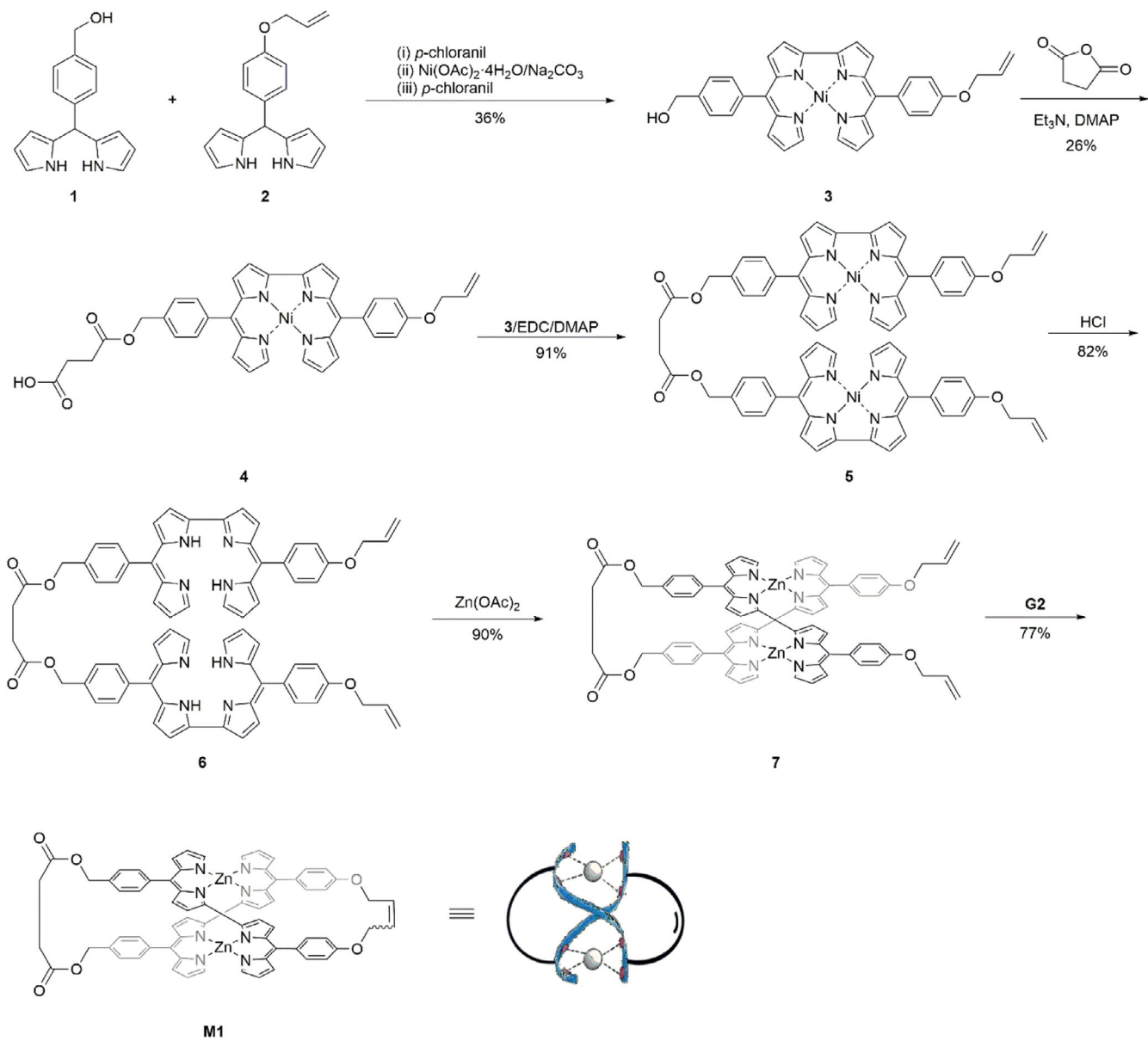
used as the monomer for ring-opening metathesis polymerization (ROMP).²¹ A polymer containing multiple BDPR-Zn units on its backbone was obtained and its mechanochemical activation under ultrasonication was tested.

2 | RESULTS AND DISCUSSION

2.1 | Design and synthesis of doubly strapped BDPR-Zn double helix monomer

As shown in Figure 2A, in order to incorporate the double helix into a polymer and have it function as a nonscissile mechanophore, the two straps on the corresponding

monomer should play two different roles: one strap serves as a linker to form a loop with the double helix so that the polymer chain is held together when the double helix is broken; on the other strap is installed an appropriate functional group for polymerization. Previously, the cyclic olefin containing BDPR-Zn (M in Figure 2B) was formed from the ring-closing metathesis (RCM) of the corresponding acyclic diene.¹⁷ The successful RCM suggests the compatibility between olefin metathesis and the BDPR-Zn double helix and the feasibility of making a BDPR-Zn-containing polymer through ROMP. Since M contains two cyclic olefins, the ROMP of which would lead to a cross-linked polymer network, we attempted to functionalize one of the alkenes through epoxidation using *meta*-chloroperoxybenzoic acid (Figure 2B); however, the helix



SCHEME 1 Synthetic route of doubly strapped double helix monomer M1

structure was decomposed under this oxidation condition, and no targeting epoxide product was obtained. We further moved to another synthetic route, in which the two straps were introduced separately (Figure 2C).

The detailed synthetic scheme of the monomer M1 is shown in Scheme 1. First, *p*-chloranil oxidation of methanol- and allyl-ether-functionalized phenyl dipyrromethanes (**1** and **2**, respectively) afforded the corresponding dipyrromethanes. To a mixture of **1** and **2** (1:1 equiv) was then added $\text{Ni}(\text{OAc})_2 \cdot 4\text{H}_2\text{O}$ for coordination, and the resulting complex was oxidized by *p*-chloranil oxidation to yield Ni (II) bidipyrin benzyl alcohol **3**. This complex is stable enough and can be purified by column chromatography without decomposition. After treating compound **3** with succinic anhydride under basic condition, Ni (II) bidipyrin carboxylic acid **4** was obtained. A Steglich esterification between **3** and **4** gave Ni (II) bidipyrin dimer complex **5**, which was demetalized under strong acidic condition to afford the linear bidipyrin dimer diene **6**. Coordination between Zn (II) and **6** yielded the singly strapped BDPR-Zn double helix diene **7**. The RCM of the diene in diluted condition led to the formation of the cyclic olefin containing doubly strapped BDPR-Zn double helix M1. We tried growing a single crystal for M1 through slow evaporation, vapor diffusion, and liquid–liquid diffusion with solvent combinations for multiple times but failed to obtain crystals that are suitable for single crystal analysis. All chemical structures of compounds were characterized by ^1H NMR spectra, UV-vis and MALDI-TOF MS (Figures S1 to S14).

As shown in Figure S9, compared with the ^1H NMR spectrum of metal-free bidipyrin dimer diene **6**, the singlet peak of two methylenes (~ 2.7 ppm) became a multiplet peak and shifted to downfield by 0.1 ppm, due to the rigidification of the twisted ethylene linker, suggesting the formation of the double helix. The characteristic peaks of allyl group (6.2, 5.4, and 5.3 ppm) disappeared in ^1H NMR spectrum of M1. Meanwhile, the appearance of a broad singlet peak (6.0 ppm) indicated the formation of a cyclic olefin. MALDI-TOF MS spectra show one set of peaks at m/z of 1130.91253.7, and 1226.3 for **6** ($[\text{C}_{72}\text{H}_{58}\text{N}_8\text{O}_6]^+$), **7** ($[\text{C}_{72}\text{H}_{54}\text{N}_8\text{O}_6\text{Zn}_2]^+$), and M1 ($[\text{C}_{70}\text{H}_{50}\text{N}_8\text{O}_6\text{Zn}_2]^+$), respectively, further confirming their molecular compositions. An obvious color change from green to blue was observed after RCM of **7** (Figure S10). The acyclic diene **7** showed an absorbance peak at ~ 425 nm, corresponding to the S mode helix; in contrast, the absorbance (Figure S10) of M1 showed a peak at ~ 570 nm, suggesting an L mode helix. The S-to-L transformation during the cyclization could be caused by the jack-effect from the resulting butene strap.¹⁷

2.2 | Synthesis and characterization of copolymer containing BDPR-Zn double helix

With the double helix monomer M1 in hand, we introduced BDPR-Zn unit into polymer backbone through copolymerization with cyclooctadiene epoxide (EP-COD). The polymerization was conducted in DCM under ambient conditions for 3 h, using Grubbs second-generation catalyst (G2) as the initiator (Figure 3A). Due to the relatively poor solubility of M1, 19/1 of EP-COD/M1 was used for the copolymerization. The copolymerization was conducted at an initial M1 concentration of 0.028 M with a M1/EP-COD/G2 feeding ratio of 1/19/0.025. The dark blue color of the reaction mixture was kept during the polymerization. Precipitation in cold method failed to purify polymer P1 due to the low solubility M1. The copolymer and unreacted M1 were separated and purified by a preparative GPC using chloroform as the eluent. The polymer showed green color, suggesting singly strapped BDPR-Zn was introduced into polymer backbone.

The copolymer was further characterized by ^1H NMR, GPC and UV-vis techniques. GPC result showed that the

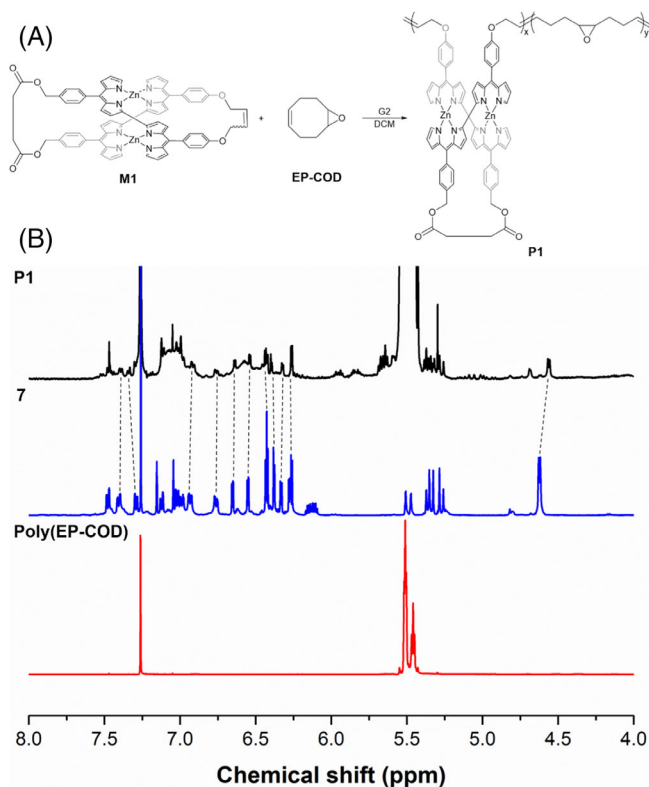


FIGURE 3 Copolymerization of M1 and EP-COD. (A) the scheme for copolymerization. (B) Partial ^1H NMR spectra for copolymer P1 (in back), acyclic BDPR-Zn diene (in blue) and EP-COD homopolymer (in red).

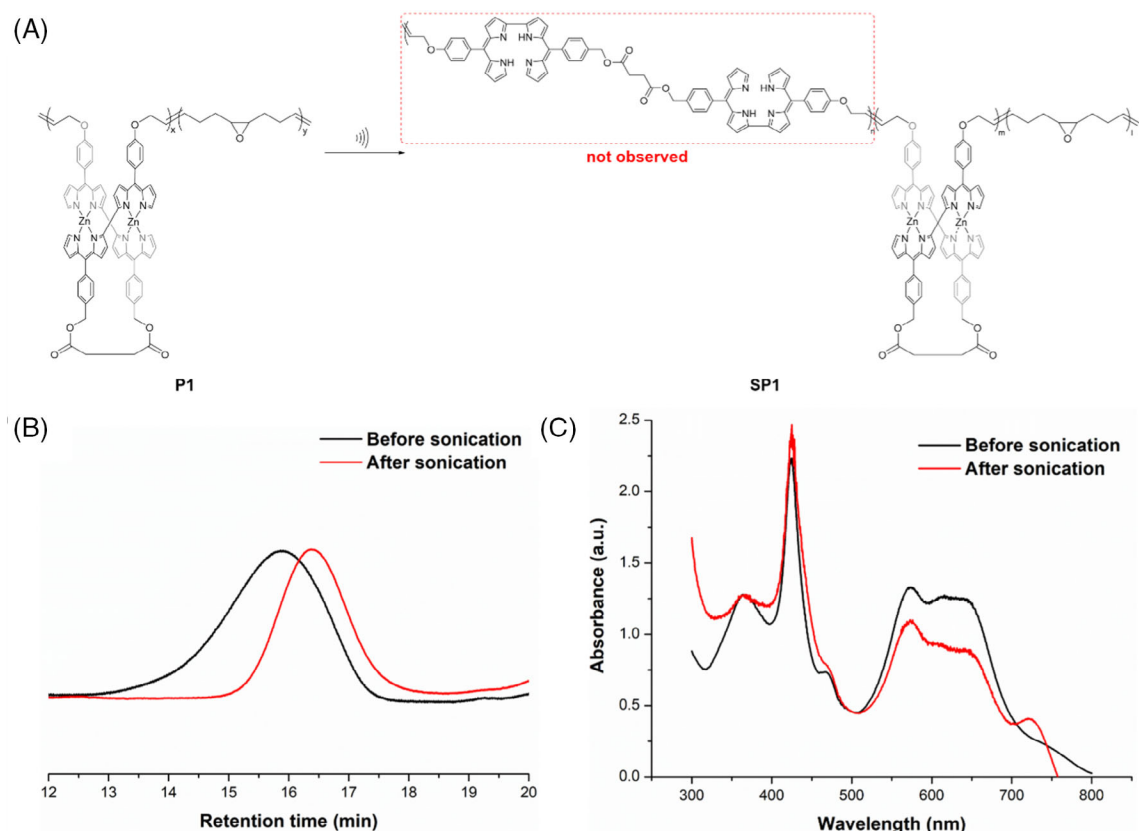


FIGURE 4 Mechanochemical testing of P1. (A) P1 is subjected to ultrasonication, resulting in SP1. (B) Partial GPC traces of P1 (black) and SP1 (red). (C) UV-vis absorption of P1 and SP1 in chloroform

number-average molecular weight (M_n) of P1 was 58 kDa with a dispersity D of 1.6. Characteristic peaks of BDPR-Zn unit can be recognized on ^1H NMR spectrum (Figure 3B), though it would be difficult to precisely quantify its content due to the low concentration. UV-vis absorption of polymer revealed a characteristic peak of *S* mode BDPR-Zn helix (Figure 4C, black curve) with the absorbance peak at ~ 425 nm, which can serve as a signal to detect the potential change in BDPR-Zn unit under mechanical force.

2.3 | Mechanochemical activation trial of BDPR-Zn double helix copolymer

In order to test the mechanochemical activation of BDPR-Zn unit, P1 with an initial M_n of 58 kDa was subjected to pulsed ultra-sonication (temperature: 6–9 °C; power density: 9.26 W cm $^{-2}$; 1 s on/1 s off). We hypothesize that as the polymer chain experiences the extensional shear force, the distance between the two Zn ions would increase, leading to the *S*-to-*L* transition, and eventually the BDPR-Zn complex would be decomposed

to release Zn (II) cation (Figure 4A), which can be detected from changes in color and UV-vis absorption of the polymer solution. After 3 h of sonication in THF, the M_n of the resulting polymer SP1 was measured to be 35 kDa (Figure 4B). However, no obvious change in the color of the polymer solution was observed during and after sonication. The absorption peak of SP1 remained at ~ 425 nm (Figure 4C), indicating that the *S* mode helix conformation in the pristine polymer P1 remained, suggesting no mechanochemical activation was observed and the drop in molecular weight is due to random chain scission of the polymer backbone under extensional shear force.^{22,23} We tried to obtain demetallized polymer as a reference, a THF solution of SP1 was treated with concentrated HCl, which led to a color change from green to light green with a green precipitate. The soluble fraction failed to provide meaningful UV-vis absorbance, suggesting polymer almost precipitated from the solution under acidic condition. The green precipitate could not be dissolved in chloroform and THF, even after it was neutralized by washing with Na₂CO₃ aqueous solution.

Since mechanochemical activation is sensitive to stereochemistry and regiochemistry and substituents on

mechanophore,²³ the linkage on helix may not be appropriate for efficient force coupling. In addition, the demetallization of BDPR-Zn often occurs in polar solvents under acidic conditions. Adjustment of the polarity or pH of the solvents used in ultrasound may also affect the results of demetallization.

2.4 | Further digging into the mechanochemical reactivity of BDPR-Zn by COGEF calculation

To further understand the mechanochemical inertness of BDPR-Zn unit, the constrained geometries simulate external force (CoGEF)²⁴ calculation was performed at semi-empirical level using PM6 model. Relaxed potential energy scans were performed where each complex was extended by pulling at two fixed atoms (or pulling points, Figure S15) incrementally with a fixed step size from a zero-force equilibrium geometry. At each step of elongation, the structure of the complex was optimized. First-order derivative of the energy with respect to the end-to-end distance was obtained to determine the force during the stepwise elongation. The energy profile showed two key steps, and each step corresponds to a Zn-N bond scission event (Figure 5). The maximum force at these steps were 4.4 and 7.8 nN, respectively, and after the second coordinate bond scission, unfolding of the helix was observed. Note that the forces required here are equivalent comparable to what is required to break a C—C bonds,^{25,26} making it difficult to mechanically unfold the helix.

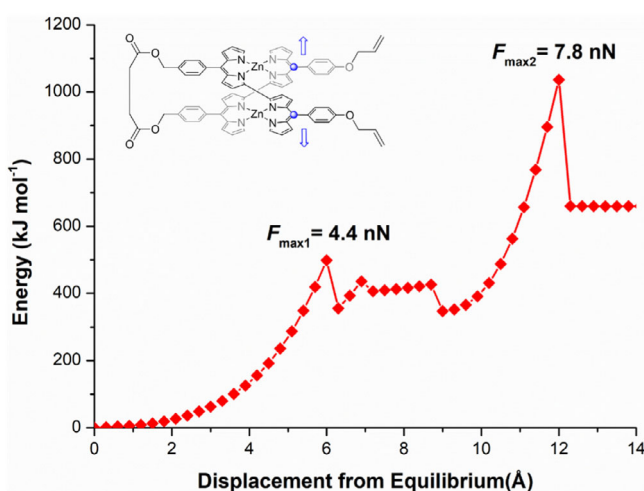


FIGURE 5 Computational simulation of BDPR-Zn unit. CoGEF calculation was performed using the PM6 semi-empirical method. The energy and the distance between pulling points were not actually zero, they were set 0 kJ/mol and 0 Å as the reference.

3 | CONCLUSION

Doubly strapped BDPR-Zn exhibits unique double helical structure and spring-like behavior. Through rational design of two straps of helix, cyclic olefin monomer containing BDPR-Zn double helix was prepared. ROMP of the monomer allows BDPR-Zn units to be introduced into polymer backbone. Pulsed ultrasonication experiments shows mechanochemical inertness of BDPR-Zn unit. Possible reasons of this phenomena were extracted and further supported by COGEF simulation results. The study presented here can inspire future efforts on the design of helix structure for mechanical unfolding.

4 | EXPERIMENTAL SECTION/METHODS

The experimental details of synthesis doubly strapped double helix monomer M1 and its copolymer P1 were included in Data S1.

Sonication experiments: Ultrasonication was conducted by using a Vibracell model VCX500 (Sonics & Materials) instrument with a standard solid probe (tip diameter = 13 mm, titanium alloy Ti-6Al-4 V) operated at 20 kHz. The P1 solution was prepared a solution with a concentration of 1 mg/1 ml in THF (stabilized with BHT). The P1 solution was transferred to a reaction vessel and then degassed by bubbling through nitrogen for half an hour. The solution was sonicated under nitrogen by using a pulse sequence 1 s on/1 s off with the energy density of 9.3 W/cm² (AMPL = 25%) in an ice bath. After sonication, the P1 solution was analyzed by UV-vis and GPC.

Computational experiments: CoGEF calculations were performed in the framework of the software Gaussian 16 on the PSC bridges supercomputer using PM6 semi-empirical method. Input structure for complex created by modifying structure coordinates for compound **1a** in the reported research.¹³ The energy and the distance between pulling points of initial unconstrained geometry were set as 0 kJ/mol and 0 Å, respectively. The distance between two carbon atoms in gray blue on meso-aryl group was set as pulling points (Figure S15) at the unconstrained geometry and then increased in 0.3 Å each step. The constrained geometry was optimized, and the total energy was minimized at each step.

ACKNOWLEDGMENTS

This material is based upon work supported by the University of Akron and National Science Foundation under grant no. CHE-2204079. The computational resources were provided by Extreme Science and Engineering

Discovery Environment (TG-CHE220003). We thank K. Williams-Pavlantos, S. Snyder, and C. Wesdemiotis for mass spectrometry analysis.

ORCID

Junpeng Wang  <https://orcid.org/0000-0002-4503-5026>

REFERENCES

- [1] L. Pauling, R. B. Corey, H. R. Branson, *Proc. Natl. Acad. Sci. U. S. A.* **1951**, *37*, 205.
- [2] J. D. Watson, F. H. C. Crick, *Nature* **1953**, *171*, 737.
- [3] T. Nakano, Y. Okamoto, *Chem. Rev.* **2001**, *101*, 4013.
- [4] Z.-M. Shi, J. Huang, Z. Ma, X. Zhao, Z. Guan, Z.-T. Li, *Macromolecules* **2010**, *43*, 6185.
- [5] K. A. Miller, O. J. Dodo, G. P. Devkota, V. C. Kirinda, K. G. E. Bradford, J. L. Sparks, C. S. Hartley, D. Konkolewicz, *Chem. Commun.* **2022**, *58*, 5590.
- [6] E. Yashima, K. Maeda, Y. Furusho, *Acc. Chem. Res.* **2008**, *41*, 1166.
- [7] F. Devaux, X. Li, D. Sluysmans, V. Maurizot, E. Bakalis, F. Zerbetto, I. Huc, A.-S. Duwez, *Chem* **2021**, *7*, 1333.
- [8] H. Zhang, C. E. Diesendruck, *Angew. Chem. Int. Ed.* **2022**, *61*, e202115325.
- [9] M. J. Narcis, N. Takenaka, *Eur. J. Org. Chem.* **2014**, *2014*, 21.
- [10] D. Becart, V. Diemer, A. Salaun, M. Oiarbide, Y. R. Nelli, B. Kauffmann, L. Fischer, C. Palomo, G. Guichard, *J. Am. Chem. Soc.* **2017**, *139*, 12524.
- [11] E. Yashima, N. Ousaka, D. Taura, K. Shimomura, T. Ikai, K. Maeda, *Chem. Rev.* **2016**, *116*, 13752.
- [12] G. Q. Yin, S. Kandapal, C. H. Liu, H. Wang, J. Huang, S. T. Jiang, T. Ji, Y. Yan, S. Khalife, R. Zhou, L. Ye, B. Xu, H. B. Yang, M. P. Nieh, X. Li, *Angew. Chem. Int. Ed.* **2021**, *60*, 1281.
- [13] Y. Zhang, Y. Zhong, A. L. Connor, D. P. Miller, R. Cao, J. Shen, B. Song, E. S. Baker, Q. Tang, S. Pulavarti, R. Liu, Q. Wang, Z. L. Lu, T. Szyperski, H. Zeng, X. Li, R. D. Smith, E. Zurek, J. Zhu, B. Gong, *J. Am. Chem. Soc.* **2019**, *141*, 14239.
- [14] Y. Zhang, A. Thompson, S. J. Rettig, D. Dolphin, *J. Am. Chem. Soc.* **1998**, *120*, 13537.
- [15] M. Bröring, S. Link, C. D. Brandt, E. C. Tejero, *Eur. J. Inorg. Chem.* **2007**, *2007*, 1661.
- [16] T. Hashimoto, T. Nishimura, J. M. Lim, D. Kim, H. Maeda, *Chem. Eur. J.* **2010**, *16*, 11653.
- [17] H. Maeda, T. Nishimura, R. Akuta, K. Takaishi, M. Uchiyama, A. Muranaka, *Chem. Sci.* **2013**, *4*, 1204.
- [18] S. A. Baudron, H. Ruffin, M. W. Hosseini, *Chem. Commun.* **2015**, *51*, 5906.
- [19] F. Zhang, S. A. Baudron, M. W. Hosseini, *New J. Chem.* **2018**, *42*, 6997.
- [20] F. Zhang, A. Fluck, S. A. Baudron, M. W. Hosseini, *Dalton Trans.* **2019**, *48*, 4105.
- [21] A. K. Pearce, J. C. Foster, R. K. O'Reilly, *J. Polym. Sci., Part A: Polym. Chem.* **2019**, *57*, 1621.
- [22] A. T. Ponomarenko, A. R. Tameev, V. G. Shevchenko, *Polymer* **2022**, *14*, 604.
- [23] N. Willis-Fox, E. Rognin, T. A. Aljohani, R. Daly, *Chem* **2018**, *4*, 2499.
- [24] I. M. Klein, C. C. Husic, D. P. Kovacs, N. J. Choquette, M. J. Robb, *J. Am. Chem. Soc.* **2020**, *142*, 16364.
- [25] K. Martin, H. Beyer, Clausen-Schaumann, *Chem. Rev.* **2005**, *105*, 2921.
- [26] S. Grimme, J. Antony, S. Ehrlich, H. Krieg, *J. Chem. Phys.* **2010**, *132*, 7307.

SUPPORTING INFORMATION

Additional supporting information can be found online in the Supporting Information section at the end of this article.

How to cite this article: J. Zhou, D. Sathe, A. Ciccotelli, J. Wang, *J. Polym. Sci.* **2023**, *61*(15), 1547. <https://doi.org/10.1002/pol.20220579>